JMEPEG (2020) 29:1544–1549
https://doi.org/10.1007/s11665-020-04667-3

1059-9495/$19.00

Effect of Laser Shock Peening on the Microstructure and Properties of the Inconel 625 Surface Layer

Magdalena Rozmus-Górnikowska, Jan Kusiński, and Łukasz Cieniek

(Submitted August 19, 2019; in revised form January 21, 2020; published online February 19, 2020)

The aim of this work was to investigate the influence of laser shock peening on the topography, microstructure, surface roughness and the mechanical properties of the Inconel 625 nickel alloy. Examination of the topography and microstructure of the nickel alloy after laser treatment was carried out by means of scanning electron microscopy as well as atomic force microscopy. The roughness of the surface was measured by WYKO NT9300 equipment. Nanohardness test was carried out using a nanoindenter NHT 50-183 of CSM Instruments equipped with a Berkovich diamond indenter. Additionally, transmission electron microscopy was used to examine the microstructural changes on the surface layer after laser treatment. The investigations showed that the laser process produced an ablation and melting of the surface layer and, hence, increased the surface roughness of the Inconel 625. On the other hand, the presence of the slip bands on the surface and on the cross section of the treated material, a high density of dislocations and a higher hardness of the treated region indicated that the laser shock processing caused severe plastic deformation of the surface layer. Additionally, due to the high plastic deformation, cracking of the carbide precipitates was observed.

Keywords Inconel 625, laser shock peening (LSP), microstructure, nanohardness, surface roughness

1. Introduction

Laser shock peening (LSP) also known as laser shock processing is an innovative laser-based surface processing technique used to modify the surface of a metallic material, which causes compressive residual stresses and microstructural changes on the surface and within the depth of the metal (Ref 1-4). Often, LSP is used to treat many aerospace products, such as turbine blades, rotor components, disks, gear shafts and bearing components (Ref 5, 6).

In the LSP process, a laser beam hits the sacrificial coating on the surface of the metallic target and forms plasma, which rapidly expands and generates shock waves into the bulk (Ref 7, 8). These shock waves induce compressive residual stresses into the metal and improve its fatigue life, which is very important in applications such as turbine blades of aircraft engines. When the induced compressive residual stresses reach the yield strength of the treated metal, plastic deformation occurs.

This article is an invited submission to JMEP selected from presentations at The XXII Physical Metallurgy and Materials Science Conference: Advanced Materials and Technologies (AMT 2019) held June 9-12, 2019, in Bukowina Tatrzańska, Poland, and has been expanded from the original presentation.

Magdalena Rozmus-Górnikowska, Jan Kusiński, and **Łukasz Cieniek**, Faculty of Metals Engineering and Industrial Computer Science, AGH University of Science and Technology, al. Mickiewicza 30, 30-059 Kraków, Poland. Contact e-mail: rozmus@agh.edu.pl.

The main advantages of the LSP process are a greater residual compressive stress depth when compared to traditional mechanical shot peening and more flexibility in process control parameters. Furthermore, it is possible to apply LSP to only selected regions of a component, because of the ability to precisely control the position of the laser (Ref 9, 10). In the aerospace industry, LSP is an effective method to improve the mechanical properties and fatigue lives of key aerospace products, such as turbine blades and rotor components (Ref 11).

Nickel-based superalloys have excellent mechanical properties, especially at medium and high temperatures (Ref 12, 13). These properties make nickel alloys widely used in aero-engine applications, such as turbine disks and blades. Therefore, many researchers have focused on mechanical properties, microstructure and fatigue life of the surface layer of nickel alloys induced by various methods such as mechanical shot peening (Ref 14, 15). However, there have been a limited number of studies carried out to understand the influence of LSP process on microstructure and properties of nickel alloys (Ref 16-18). For example, Li et al. (Ref 16) studied the aero-engine turbine blade nickel K417 alloy and observed the microstructural change on the surface of the nickel-based alloy after LSP treatment. The authors demonstrated that a primary feature of the LSP strengthening mechanism in this nickel-based alloy is the synergistic effect of the nanocrystalline surface and the residual compressive stress. The residual stress relaxes with increasing annealing time (up to 150 min) at 530, 700 and 900 °C for 150 min, but still remains adequately compressive at levels of 482, 347 and 161 MPa, respectively. Wang et al. (Ref 17) investigated the effects of LSP on microstructure and mechanical properties of K403 nickel alloy. The authors showed that after LSP of the K403 nickel alloy, the microhardness and residual stress were improved in a plastic deformation layer. Additionally, with increasing numbers of laser impacts, the effective depth of hardness and residual stress was also improved. Moreover, the authors revealed that the fatigue lives of samples subjected to three impacts increased by 244%. Nath

et al. (Ref 18) studied the effect of LSP on the phase, residual stress and hardness of Hastelloy X superalloy. The authors studied the influence of the absorptive coating type on the stress level. They showed that tensile stresses were developed in the Hastelloy X superalloy when they were subjected to LSP without any absorptive layer. On the other hand, compressive residual stresses of 48 to 166 MPa were developed on the surface of Hastelloy X superalloy when they were laser shock peened with the aforementioned absorptive layers. A maximum compressive residual stress of 166 MPa was observed on the Hastelloy X superalloy when laser shock peened with an Al absorptive layer. Strain hardening was increased on the samples treated with an Al absorptive layer compared to a black vinyl tape. A maximum hardness of around 380 VHN was found with an Al absorptive layer compared to that of around 360 VHN for a black vinyl tape. However, they showed that dislocation densities were higher when the samples were laser shock peened without an absorptive layer, implying a higher plastic deformation in the sample.

Studies on LSP of the Inconel 625 superalloy were primarily focused on the mechanical properties and residual stress development. Karthnik and Stango analyzed the effect of LSP on mechanical properties, roughness of the surface, residual stresses and corrosion behavior of the Inconel 625 after LSP (Ref 19). Little or even no emphasis in the literature has been placed on a detailed microstructural characterization by TEM for this type of alloy system after laser treatment.

This paper describes how the topography, microstructure, surface roughness and mechanical properties (nanohardness) of the Inconel 625 nickel alloy are affected by LSP.

2. Materials and Experimental Procedures

The investigations were performed on the solid-solution-strengthened Inconel 625 alloy in the wrought condition. The microstructure of the Inconel 625 before treatment was composed of carbides uniformly distributed in the γ-austenite substrate. The chemical composition of the Inconel 625 is given in Table 1. Before laser treatment, the surface of the investigated material was ground and polished to make the surface roughness Ra = 100 nm. Next, surfaces were coated with black paint as a laser-energy-absorbing layer and then immersed in water. Flowing water was used as a confining medium, and black paint was used as the sacrificial ablative coating.

For this application, a nanosecond Nd:YAG laser (Q-switched Powerlite Precision II 9010 DLS) operating in the 1064-nm wavelength range (first harmonic) and at a frequency of 10 Hz was used in the experiment. During the LSP process, the Inconel 625 sample was treated by a series of single laser shots. The diameter of the laser beam on the target was 4 mm, whereas the laser power density was 10 J/cm^2. After LSP, the remaining black paint coating was stripped off with acetone.

The topography of the laser-treated surfaces and cross sections of the microstructure from the treated samples were examined by means of scanning electron microscopy (SEM, Hitachi S-3500 N) as well as atomic force microscopy (AFM, Veeco Dimension®Icon™ SPM). To precisely characterize the microstructure of the LSP-treated region, transmission electron microscopy observations were utilized (TEM, Philips CM20 and JEOL 200CX). Thin foils were prepared by mechanical grinding on the untreated sides to obtain thin plates. The disk centers were then dimpled down to 30-50 μm (also from the untreated substrate side). Finally, samples were electropolished to make them suitable for TEM observations.

Additionally, optical interferometry (Veeco Wyko NT 9300 profilometer) was used to examine surface roughness and the condition of the surface before and after LSP treatment. Measurements of surface roughness were repeated three times at each region.

Moreover, after the LSP treatment, nanohardness tests were conducted on the cross sections of the treated sample surfaces as well as the untreated material. Nanoindentation tests were performed using nanoindenter NHT 50-183 of CSM Instruments equipped with a Berkovich diamond indenter. Tests included cross-sectioned measurements with a step size of 5 μm, along the line perpendicular to the surface treated by LSP. A load of 15 mN was applied for each indentation.

3. Results and Discussion

A detailed analysis of the microstructure after LSP process was performed using SEM images of the surface. Figure 1 shows the topography of the investigated Inconel 625 alloy after laser shock processing. Even though the sample surfaces were coated with the absorbing layer (the black paint) to protect the surface of the material from direct ablation and to promote a better coupling with the laser energy, the SEM images of the treated material showed that similar to our previous studies concerning LSP, the laser treatment caused melting and ablation of the surface layer of the investigated material (Ref 2, 4).

The features most frequently observed on the surface after the LSP process appear as craters, holes and solidified droplets. They are most likely caused by material ablation during the process. However, a closer look at the laser-irradiated surface revealed the formation of a high density of slip bands (Fig. 1). Additionally, slip bands were clearly visible on the cross section of the treated material after treatment in the near-surface region. The cross-sectional SEM image of the Inconel 625 after LSP is presented in Fig. 2. Furthermore, the presence of slip bands was also confirmed by AFM. Figure 3 illustrates the AFM image of the Inconel 625 sample surface after LSP with a visible high density of slip bands (scanning area: 70 μm × 70 μm). One of the interesting research findings is that cracking of carbides was observed after the LSP process both on the surface

Table 1 Chemical composition of Inconel 625 samples, wt.%

Alloy	Cr	Mo	Nb	Fe	Mn	Si	Al	C	Ni
Inconel 625	22.24	9.14	3.46	0.31	0.01	0.07	0.07	0.02	Balance

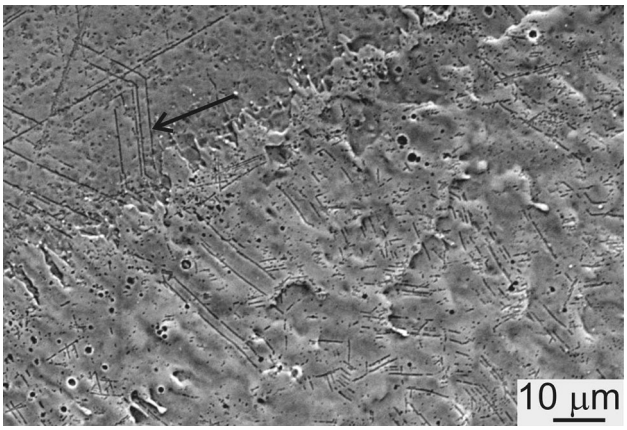

Fig. 1 SEM image showing topography of the Inconel 625 sample after LSP with a visible high density of slip bands

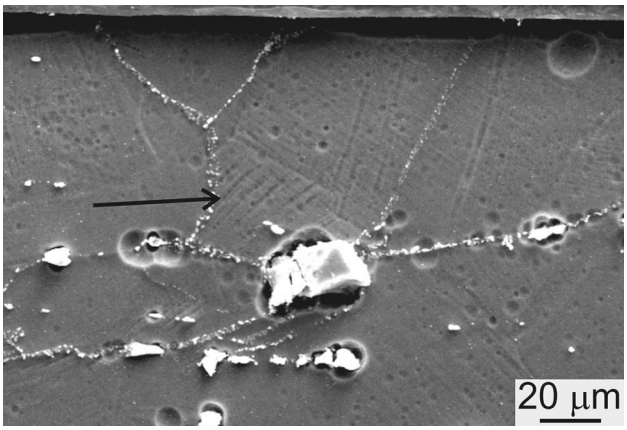

Fig. 2 SEM cross-sectional image of the treated material; an arrow indicates the area with a high density of slip bands

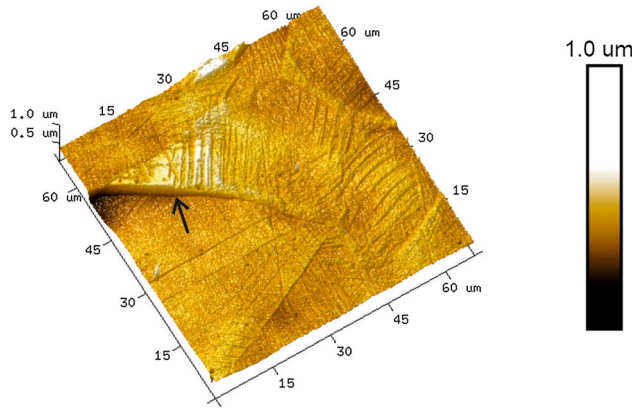

Fig. 3 AFM image showing topography of the Inconel 625 sample after LSP with a visible high density of slip bands

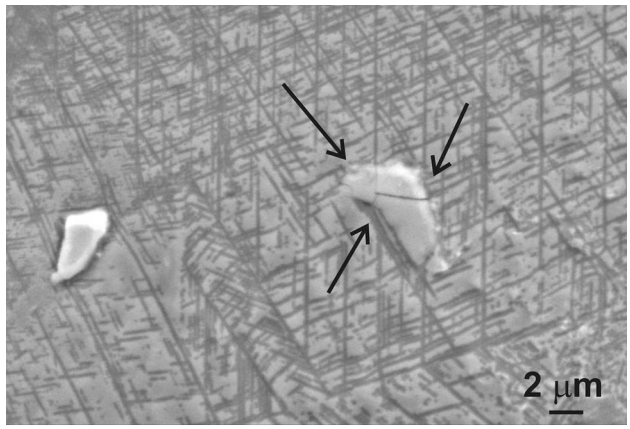

Fig. 4 SEM image showing carbide precipitate; arrows indicate visible cracks

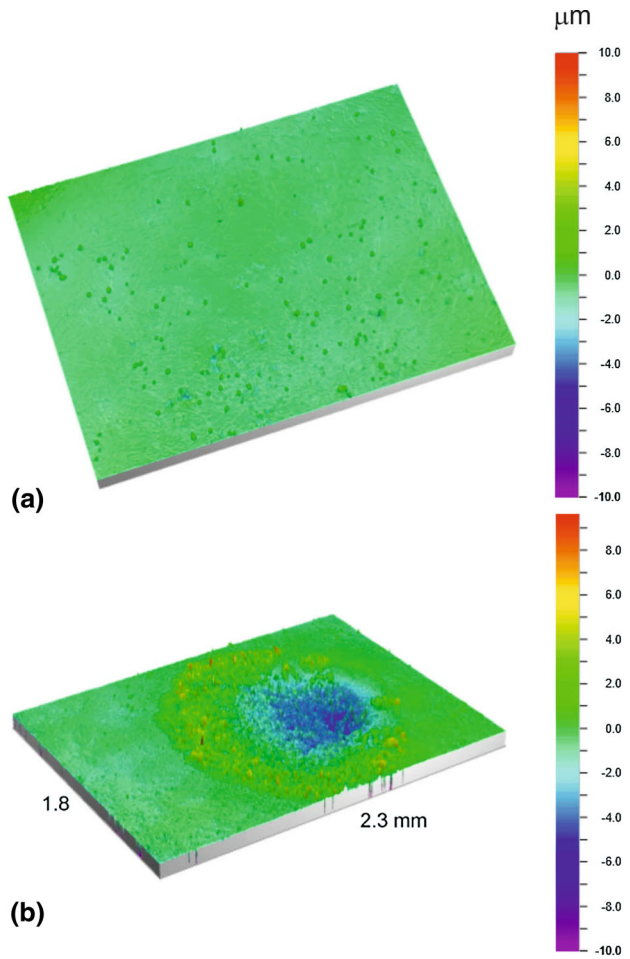

Fig. 5 3D profile of surface roughness of the Inconel 625 before (a) and after (b) laser treatment

and on the cross section of the treated material. SEM images show that cracks appear in carbides on the extension of the slip bands, as indicated by the arrows in Fig. 4.

According to literature data (Ref 2, 8), in metallic materials such as steel, aluminum or titanium alloys with relatively good ductility and fracture toughness, LSP process has been successfully used to improve fatigue, wear and stress corrosion cracking resistance. However, in brittle materials such as oxides or carbides, LSP has not been widely used, and the effect of this process on these materials is still poorly understood. Zhang et al. (Ref 9, 20) investigated laser shocking of Al_2O_3 ceramics and further studied the fracture morphology that formed from the strong laser shock processing. It was found that brittle fracture occurred at a laser pulse energy of 42 J. When the laser

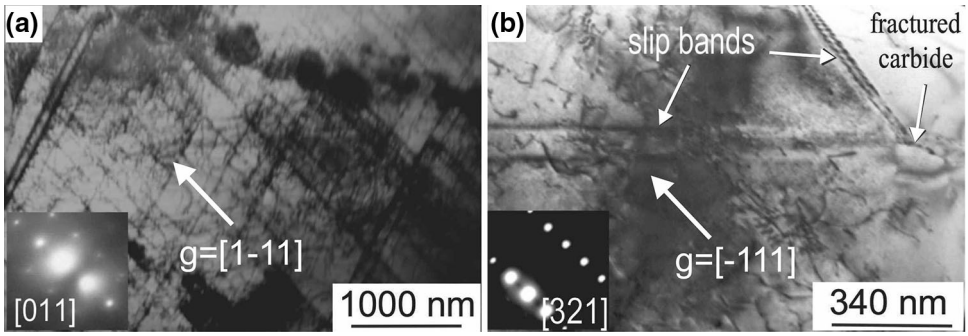

Fig. 6 TEM bright-field image (a) showing microstructure of the Inconel 625 after LSP process (TEM) as well as the corresponding diffraction pattern (b)

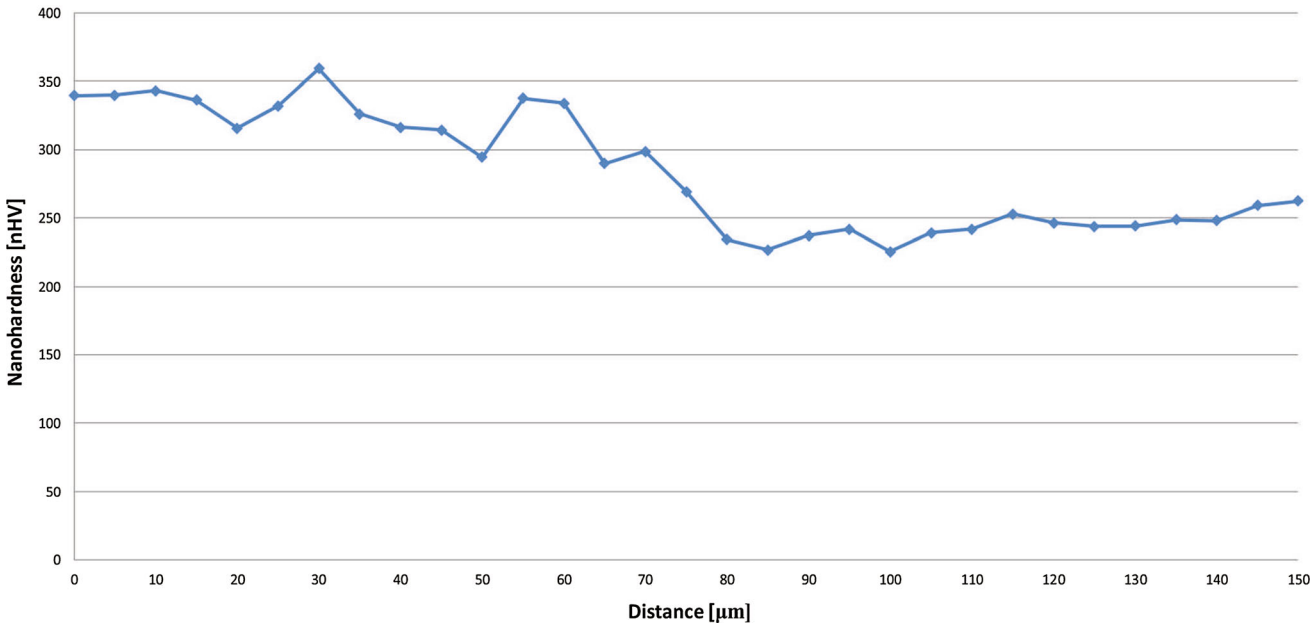

Fig. 7 Nanohardness of the treated sample as a function of a depth

energy was reduced to 25 J, the brittle fracture of ceramics appears to be comprised of plastic deformation (Ref 9, 20). Probably, cracking of carbides in the investigated material occurs due to large plastic deformation, but one should remember that the consequence of the cracking of carbides may be the concentration of high compressive stress levels in their vicinity.

The surface roughness of the material was measured for both the untreated and the laser-shock-peened nickel alloys. The average roughness Ra (arithmetic average of the absolute values of the profile height deviations from the mean line) increased from 100 nm before treatment to 1 µm after LSP process. Figure 5 shows the 3D optical surface profile images of the untreated (a) and treated (b) samples. It is evident [and consistent with the literature (Ref 4, 5)] that the LSP treatment increases the roughness of the surface. The increase in surface roughness is a consequence of the combined effect of the laser pulse pressure and the ablative nature of the laser process.

Typical TEM images of the near-surface microstructure of the specimen treated by LSP are shown in Fig. 6(a) and (b). The dense slip bands (Fig. 6a) formed under the dynamic conditions characteristic to LSP indicate that the formation of slip bands is easier under high-strain-rate conditions, which show qualitative agreement with cross-slip simulations made by Wang et al. (Ref 21). Figure 6(b) shows a fractured carbide particle (arrowed) stopping the crossing slip bands at an angle of 60°. It seems that the plastic deformation level reached a threshold value, fracturing the marked carbide. The crossing slip bands associated with precipitate shearing would be expected to give rise to crack initiation.

The TEM micrographs reveal a remarkably high density of dislocations. Similar observations were made by other investigators (Ref 16, 22-25). Ren et al. (Ref 22) noted that LSP generated high-density dislocations and improved the mechanical properties of aluminum alloys. Yan et al. (Ref 25) indicated that a high density of dislocations, stacking faults and deformations twins were generated in oxide dispersion-strengthened austenitic steels after LSP.

The nanohardness values of the Inconel 625 measured on the polished cross sections without LSP treatment were approximately 270 HV. After the LSP process, the nanohardness measured near the surface increased to a value 350 HV. A

40% increase in hardness is associated with the high density of dislocations generated in the surface region in the irradiated spot during the LSP process as well as a high density of slip bands. The graph illustrating the variation of the nanohardness of the sample as a function of a depth is presented in Fig. 7. As the depth exceeds 80 µm, the nanohardness tends to be constant. A similar trend that hardness increases after the LSP process was also observed in previous reports on various alloys after laser shock peening (Ref 26).

4. Conclusions

In this paper, the linkage between microstructure, deformation mode and hardness has been examined and discussed. In all cases examined, the deformation is localized within a rather large number of deformation bands. The following conclusions can be drawn from this study:

- The laser shock processing produced melting and ablation of the surface layer of the treated material; however, the presence of dense slip bands on the surface and on the cross section of the treated material as well as a high density of dislocations indicated that severe plastic deformation appears in the surface layer of investigated material after LSP process.
- Due to the plastic deformation, cracking of carbides by crossing slip bands associated with precipitate shearing was observed.
- The surface of the treated material was roughened by the LSP process.
- The values of nanohardness in the laser-shocked region were clearly higher than those in the non-shocked region. The enhancement of LSP on the nanohardness of Inconel 625 nickel alloy was mainly due to the high density of slip bands and dislocations.
- Below the surface, the shock hardening effect decreases with increasing distance from the surface.

Acknowledgments

The investigations were financed by the AGH University of Science and Technology Project 16.16.110.663 – zad.1.

References

1. A. Telang, Ch. Ye, A. Gill, S. Teysseyre, S.R. Mannava, D. Qian, and V. K. Vasudevan, Effect of Laser Shock Peening on SCC behavior of alloy 600, in *16th International Conference on Environmental Degradation of Materials in Nuclear Power System-Water Reactors*, 2013, Idaho National Laboratory
2. M. Rozmus-Górnikowska, J. Kusiński, and M. Blicharski, Laser Shock Processing of an Austenitic Stainless Steel, *Arch. Metall. Mater.*, 2010, **55**(3), p 635–639
3. X. Yi, H. Tian-tian, L. Peng-yan, C. Lu-fei, R. Feng-zhang, and A.A. Volinsky, Effect of Laser Pulse Energy on Surface Microstructure and Mechanical Properties of High Carbon Steel, *J. Cent. South Univ.*, 2015, **22**, p 4515–4520. https://doi.org/10.1007/s11771-015-3000-1
4. M. Rozmus-Górnikowska, J. Kusiński, and M. Blicharski, The Influence of the Laser Treatment on Microstructure of the Surface Layer of an X5CrNi18-10 Austenitic Stainless Steel, *Arch. Metall. Mater.*, 2011, **56**(3), p 717–721. https://doi.org/10.2478/v10172-011-0079-8
5. A.S. Gilla, A. Telang, and V.K. Vasudevan, Characteristics of Surface Layers Formed on Inconel 718 by Laser Shock Peening With and Without a Protective Coating, *J. Mater. Process. Technol.*, 2015, **225**, p 463–472. https://doi.org/10.1016/j.jmatprotec.2015.06.0260924-0136
6. R. Sundar, B.K. Pant, H. Kumar, P. Ganesh, D.C. Nagpure, P. Haedoo, R. Kaul, K. Ranganathan, K.S. Bindra, S.M. Oak, and L.M. Kukreja, Laser Shock Peening of Steam Turbine Blades for Enhanced Service Life, *Pramana J. Phys.*, 2014, **82**(2), p 347–351. https://doi.org/10.1007/s12043-014-0688-7
7. Ch Danduk, A.N. Jinoop, M.J. Yadav, and S.K. Subbu, Modeling and Strategies for Laser Shock Processing, *Mater. Today*, 2016, **3**(10), p 3997–4002. https://doi.org/10.1016/j.matpr.2016.11.063
8. ChS Montroos, T. Wei, L. Ye, G. Clark, and Y.W. Mai, Laser Shock Processing and Its Effect on Microstructure and Properties of Metal Alloys: A Review, *Int. J. Fatique*, 2002, **24**, p 1021–1036
9. P.P. Shukla, P.T. Swanson, and C.J. Page, Laser Shock Peening and Mechanical Shot Peening Processes Applicable for the Surface Treatment of Technical Grade Ceramics: A Review, *Proc IMechE Part B J Eng. Manuf.*, 2013, https://doi.org/10.1177/0954405413507250
10. R. Fabbro, P. Peyre, L. Berthe, and X. Scherpereel, Physics and Applications of Laser-Shock Processing, *J. Laser Appl.*, 1998, **6**(10), p 265–279
11. B. Lin, S. Zabeen, J. Tong, M. Preuss, and J. Withers, Residual Stresses in Due to Foreign Object Damage in Laser Shock Peened Aerofoils: Simulation And Measurement, *Mech. Mater.*, 2015, **82**, p 78–90. https://doi.org/10.1016/j.mechmat.2014.12.001
12. M. Rozmus-Górnikowska, M. Blicharski, and J. Kusiński, Influence of Weld Overlaying Methods on Microstructure and Chemical Composition of Inconel 625 Boiler Pipe Coatings, *Kovove Mater. Met. Mater.*, 2014, **52**(3), p 141–147
13. M. Rozmus-Górnikowska and M. Blicharski, Microsegregation and Precipitates in Inconel 625 Arc Weld Overlay Coatings on Boiler Pipes, *Arch. Metall. Mater.*, 2015, **60**(4), p 2599–2605. https://doi.org/10.1515/amm-2015-0420
14. K. Zaleski, A. Skoczylas, and M. Brzozowska, The Effect of the Conditions of Shot Peening the Inconel 718 Nickel Alloy on the Geometrical Structure of the Surface, *Adv. Sci. Technol. Res. J.*, 2017, **11**, p 205–211. https://doi.org/10.12913/22998624/74180
15. D. Kumar, S. Idapalapati, and W. Wie, *Microstructural Response and Strain Hardening in Deep Cold Rolled Nickel-Based Superalloy for Aerospace Application*, 2018, **71**, p 374–379. https://doi.org/10.1016/j.procir.2018.05.044
16. Y. Li, L. Zhou, W. He, G. He, X. Wang, X. Nie, B. Wang, S. Luo, and Y. Li, The Strengthening Mechanism of a Nickel Based Alloy After Laser Shock Processing at High Temperatures, *Sci. Technol. Adv. Mater.*, 2013, **14**, p 1–9. https://doi.org/10.1088/1468-6996/14/5/055010
17. C. Wang, X.J. Au, L.C. Zhou, and Y. Chai, Effects of Laser Shock Processing on Microstructures and Mechanical Properties of K403 Nickel-Alloy, *Mater. Des.*, 2016, **89**, p 582–588. https://doi.org/10.1016/j.matdes.2015.10.022
18. S. Nath, P. Shukla, X.J. Shen, and J. Lawrence, Effect of Laser Shock Peening (LSP) on the Phase Evolution, Residual Stress and Hardness of Hastelloy-X Superalloys, *Lasers Eng.*, 2018, **39**, p 97–112

19. D. Karthik, S. Arul Xavier Stango, U. Ijayalakshmi, and S. Swaroop, Electrochemical Behavior of Laser Shock Peened Inconel 625 Superalloy, *Surf. Coat. Technol.*, 2017, **311**, p 46–54. https://doi.org/10.1016/j.surfcoat.2016.12.105
20. L.F. Zhang, Y. Zhang, and A. Feng, The Fracture Microphology of the Ceramics by Strong Laser Shock Processing, *Mater. Sci. Forum*, 2006, **532–533**, p 137–140. https://doi.org/10.4028/www.scientific.net/MSF.532-533.137
21. Z.Q. Wang, I.J. Beyerlein, and R. LeSar, Slip Band Formation and Mobile Dislocation Density Generation in High Rate Deformation of Single FCC Crystals, *Philos. Mag.*, 2008, **2008**(88), p 1321–1343. https://doi.org/10.1080/14786430802129833
22. X.D. Ren, W.F. Zhou, Y.P. Ren, S.D. Xu, F.F. Liu, S.Q. Yuan, N.F. Ren, and J.J. Huang, Dislocation Evolution and Properties Enhancement of GH2036 by Laser Shock Processing: Dislocation Dynamic Simulation and Experiment, *Mater. Sci. Eng. A*, 2016, **264**, p 184–192
23. B.S. Yilbas, A.F.M. Arif, S.Z. Shuja, M.A. Gondal, and J. Shirokof, Investigation Into Laser Shock Processing, *J. Mater. Eng. Perform.*, 2004, **13**(1), p 47–54. https://doi.org/10.1361/10599490417623
24. S.G. Irizalpa, N. Saklakoglu, and B.S. Yilbas, Characterization of Microplastic Deformation Produced in 6061-T6 by Using Laser Shock Processing, *Int. J. Adv. Manuf. Technol.*, 2014, **71**, p 109–115. https://doi.org/10.1007/s00170-013-5481-0
25. X. Yan, F. Wang, L. Deng, Ch Zhang, Y.F. Lu, M. Nastasi, M.A. Kirk, M. Li, and B. Lui, Effect of Laser Shock Processing on the Microstructures and Properties of Oxide-Dispersion-Strengthened Austenitic Steels, *Adv. Eng. Mater.*, 2018, **20**, p 1–8. https://doi.org/10.1002/adem.201700641
26. G.X. Lua, J.D. Liua, H.C. Qiaob, Y.Z. Zhoua, T. Jina, J.B. Zhaob, X.F. Suna, and Z.Q. Hua, Surface Nano-hardness and Microstructure of a Single Crystal Nickel Base Superalloy After Laser Shock Peening, *Opt. Laser Technol.*, 2017, **91**, p 116–119. https://doi.org/10.1016/j.optlastec.2016.12.032